

13.5 nm **extreme ultraviolet** emission from tin based laser produced plasma sources

Cite as: J. Appl. Phys. **99**, 093302 (2006); <https://doi.org/10.1063/1.2191477>

Submitted: 03 November 2005 • Accepted: 28 February 2006 • Published Online: 11 May 2006

Paddy Hayden, Anthony Cummings, Nicola Murphy, et al.



View Online



Export Citation

ARTICLES YOU MAY BE INTERESTED IN

[Optimizing 13.5nm laser-produced tin plasma emission as a function of laser wavelength](#)
Applied Physics Letters **90**, 181502 (2007); <https://doi.org/10.1063/1.2735944>

[Comparative study on emission characteristics of extreme ultraviolet radiation from CO₂ and Nd:YAG laser-produced tin plasmas](#)
Applied Physics Letters **87**, 041503 (2005); <https://doi.org/10.1063/1.1989441>

[Characterization of extreme ultraviolet emission from laser-produced spherical tin plasma generated with multiple laser beams](#)
Applied Physics Letters **86**, 051501 (2005); <https://doi.org/10.1063/1.1856697>



APL Quantum

CALL FOR APPLICANTS

Seeking Editor-in-Chief

13.5 nm extreme ultraviolet emission from tin based laser produced plasma sources

Paddy Hayden,^{a)} Anthony Cummings, Nicola Murphy, Gerry O'Sullivan, Paul Sheridan, John White, and Padraig Dunne

School of Physics, University College Dublin, Belfield, Dublin 4, Ireland

(Received 3 November 2005; accepted 28 February 2006; published online 11 May 2006)

An examination of the influence of target composition and viewing angle on the extreme ultraviolet spectra of laser produced plasmas formed from tin and tin doped planar targets is reported. Spectra have been recorded in the 9–17 nm region from plasmas created by a 700 mJ, 15 ns full width at half maximum intensity, 1064 nm Nd:YAG laser pulse using an absolutely calibrated 0.25 m grazing incidence vacuum spectrograph. The influence of absorption by tin ions (Sn I–Sn X) in the plasma is clearly seen in the shape of the peak feature at 13.5 nm, while the density of tin ions in the target is also seen to influence the level of radiation in the 9–17 nm region. © 2006 American Institute of Physics. [DOI: 10.1063/1.2191477]

I. INTRODUCTION

Progress towards the fabrication of semiconductor structures at the 32 nm node and beyond requires the development of a source of extreme ultraviolet (EUV) radiation compatible with the multilayer optics currently envisaged for use in photolithography tools. The high reflectivity ($\sim 70\%$) of molybdenum silicon (Mo/Si) multilayer mirrors¹ at 13.5 nm dictates that the source must be bright at this wavelength. The bandpass for a system of these mirrors is typically 2% at 13.5 nm, thus one key challenge facing source designers is to optimize the EUV flux emitted by the source in this range. The elements tin, xenon, and lithium appear suitable as candidates for such a plasma-based source. In the case of tin the emission in the EUV is from 8 to 13 times ionized species in the plasma,^{2–4} while only 10 times ionized xenon emits at 13.5 nm.^{5,6} Interest has been shown in xenon principally due to its usefulness in a range of plasma configurations^{7–9} and the inherent cleanliness of inert gaseous sources. However, tin based targets have the potential to provide a higher conversion efficiency (CE) owing to the range of ions that contribute to emission in the 2% band centered at 13.5 nm.

The EUV radiation emitted from a laser produced plasma (LPP) is unlikely to be isotropic for most target schemes illuminated from one side only^{9–14} and is certainly not the case where the plasma is formed from a planar solid target. As the maximum collection angle of the primary optic in the EUV exposure tool is likely to be in the range of $1.8\text{--}2\pi$ sr,¹⁵ both the orientation of the solid target surface and illuminating laser axis to that optic will greatly influence the level of collectable EUV radiation.

II. BACKGROUND

This paper reports work concentrated on LPPs formed from three types of bulk solid targets: pure tin foil, a ceramic containing 5% tin atoms by number, and a second ceramic

containing 6% tin atoms by number. It addresses three aspects: (1) the effect that the percentage of tin in the target has on the EUV spectrum, (2) the effect of incident laser power density on the EUV spectrum, and (3) the influence of the viewing angle on the observed spectrum and the inferred CE. A steady state collisional-radiative (CR) model¹⁶ is used to identify the ionization balance and laser pulse power density that optimizes the EUV inband output at 13.5 nm, as previously reported by White *et al.*¹⁷ The CR model of the plasma describes situations where both electron collisions and radiative transitions are responsible for recombination and deexcitation processes. It provides a steady state ionization balance within the plasma as a function of both the target element atomic number (Z) and the incident laser pulse power density. Thus the CR model predicts plasma conditions where a relatively narrow distribution of ions prevails at moderate incident laser pulse power densities. The emission characteristics of the relevant ions are obtained from atomic structure calculations made with the HFCI (Hartree-Fock with configuration interaction) code of Cowan,¹⁸ which explicitly accounts for configuration interaction between those configurations provided in the input. In addition, it is possible to account for other interactions by scaling the Slater-Condon integrals from their *ab initio* values by 50%–150%. The calculations used to analyze the spectra presented here employed a scaling of the order of 60%–99%.

It is well established that $4p\text{--}4d$ and $4d\text{--}4f$ transitions from a range of ion stages of atoms with $50 < Z < 70$ combine to form an unresolved transition array (UTA), comprising perhaps millions of individual lines and dominating the EUV region of the spectrum.^{19–21} The UTA in the EUV spectrum of tin, formed by transitions of the type $4p^6 4d^k 4f^n \rightarrow 4p^5 4d^{k+1} 4f^n + 4d^{k-1} 4f^{n+1} + 4d^{k-1} 4f^n 5p$ from the ions 8^+ through 13^+ , is centered at 13.5 nm, while the corresponding feature in the spectrum of xenon is found at 11 nm.^{6,22} The UTA is quite broad [2–3 nm full width at half maximum (FWHM)] in the spectrum of pure tin. Matsui and Kogawa²³ and Choi *et al.*¹¹ recorded the spectrum of SnO_2 and SnO , while O'Sullivan and Faulkner⁴ recorded the spectra of tin

^{a)}Electronic mail: patrick.hayden@ucd.ie

doped compounds and found that as the percentage of tin in an otherwise low-Z target is reduced to a few percent, the FWHM of the UTA gradually narrows to about 0.3 nm.⁴ It was also found that combining a low percentage of high-Z elements in a target of predominantly low-Z materials greatly reduced the level of plasma recombination radiation emitted by the target.²⁴ In the context of the reflective optics envisaged for the EUV lithography (EUVL) tools this broadband recombination radiation does not contribute to the brightness of the LPP source; indeed, it poses a potential problem, leading to heating of the reflective optics, or, at longer wavelengths, causing flare in the exposure tool.²⁵

Kauffman *et al.*²⁶ achieved a CE of 1% using 7.5 ns, 300 mJ frequency doubled Nd:YAG (yttrium aluminum garnet) pulses ($\lambda=532$ nm). They observed that the CE was highly sensitive to the incident laser pulse power density and that it peaked at a power density of 2×10^{11} W cm⁻². Shevelko *et al.*²⁷ recorded a peak CE into a 1% bandwidth at 13.5 nm of 0.31% with 800 mJ, 28 ns krypton fluoride laser pulses ($\lambda=248$ nm) incident on a pure tin target at a power density of 1×10^{12} W cm⁻². Koay *et al.*²⁸ reported conversion efficiencies of up to 5% into the 2% bandwidth from solid tin targets into 2π sr, based on measurements made at 30° to the laser axis from a 1.6 J, 11.5 ns Nd:YAG laser pulse. Myers *et al.*²⁹ reported a conversion efficiency of almost 3% from a lithium target. In none of these recent reports are the reported CEs based on measurements made over a range of angles.

III. EXPERIMENTAL DETAILS

The targets used in this work were either pure tin or ceramics containing 5% or 6% tin atoms by number. The ceramics were based on SiO₂ and Spectraflux[®] mixed with varied amounts of SnO₂ and fired in a pipe furnace at temperatures between 900 and 1250 °C. The samples were ground and refired to improve homogeneity, structure, and hardness, and a flat surface was machined before the samples were mounted into the target chamber. Shot to shot variations were not found to be significant and scanning electron microscopy (SEM) revealed the inhomogeneities to be insignificant on the scale of the laser pulse diameter. The percentage tin composition was ascertained after target fabrication by x-ray fluorescence (XRF).

The source plasma was formed by the irradiation with 700 mJ pulses from a 5 Hz Nd:YAG laser, operating at the fundamental wavelength of 1064 nm, and was focused at normal incidence onto solid slab targets by planoconvex BK7 glass lenses. The laser pulse energy at the target plane was measured using a Litron LM301 photodiode based energy monitor with a calibrated accuracy of 3%. The temporal profile of the pulses was not Gaussian due to the longitudinal mode structure of the cavity. To estimate the spot size, the laser pulse was focused onto a polished silicon wafer and the diameter of the resultant crater was measured with a traveling microscope. The position of the focusing lens was monitored using a Heidenhain gauge thus ensuring reproducibility

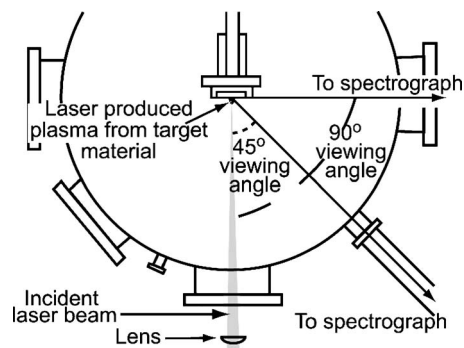


FIG. 1. Schematic of target chamber used, showing the 45° and 90° viewing angles. The laser pulse is incident along the target normal.

of focus. The power density of the focused laser pulse could be varied by either changing the focusing condition or the pulse energy.

The spectra were recorded on an absolutely calibrated Jenoptik 0.25 m flat field grazing incidence spectrometer equipped with a piezoelectric entrance shutter and a backside illuminated charge couple device (CCD) detector. With a 36 μ m entrance slit the resolution ($\lambda/\Delta\lambda$) at 13.5 nm is approximately 1300. The spectral range of the instrument is 9–17 nm and the 2% band centered at 13.5 nm occupies 33 pixels along the spectral dimension of the CCD. The source plasma lies along the optic axis of the spectrometer while the plasma expansion axis was at either 45° or 90° to the optic axis, as shown in Fig. 1.

IV. RESULTS AND DISCUSSION

Figures 2 and 3 show single shot EUV spectra recorded from plasmas formed from pure tin targets and ceramic targets containing 5% tin atoms by number. Over approximately 5 shots the spectra were not found to change significantly. The power density on the target was estimated to be 1.6×10^{11} W cm⁻² in the case of spectra of plasmas formed from pure tin targets and 1.9×10^{11} W cm⁻² for those spectra recorded from ceramic targets. The dramatic difference in the nature of the spectra formed from the two types of targets is clearly evident. The level of continuum emitted by the ceramic targets is much reduced in comparison with the pure tin case. This is due to the reduced average level of ionization in the plasma, leading to lower levels of recombination

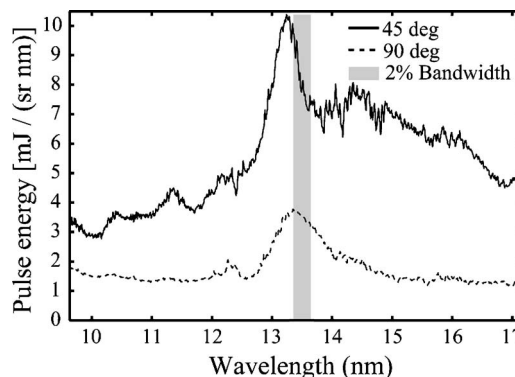


FIG. 2. Emission spectra of plasmas formed from solid tin targets, viewed at angles of 90° and 45° from the laser pulse illumination axis.

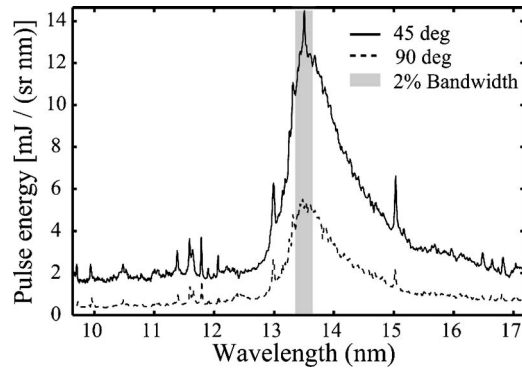


FIG. 3. Emission spectra of plasmas formed from ceramic targets containing 5% tin atoms, viewed at angles of 90° and 45° from the laser pulse illumination axis.

and bremsstrahlung emission.²⁴ Indeed, if the spectral efficiencies ($\eta = E_{13.5 \text{ nm} \pm 1\%} / E_{9-17 \text{ nm}}$) are compared one can see that the inband energy is 6% of the total EUV energy collected for the pure target and 12% in the case of the 5% tin target.

A second notable feature is the increased spectral brightness in both cases when the plasma is viewed at 45°, as compared to the 90° case. In the case of the pure tin target, the inband emission increases from 5.7 to 14 mJ/sr/nm and the peak of the UTA shifts to a shorter wavelength outside the 2% bandwidth, in agreement with the findings of Choi *et al.*¹¹ For the ceramic target, the increase in inband emission is from 8.3 to 22 mJ/sr/nm; however, there is no shift in peak wavelength. As noted by Filevich *et al.*,³⁰ the EUV emission from the plasma itself ablates material from the surrounding solid target, forming a dense, cool plasma (temperature of 1–4 eV) in the region close to the target surface. This results in the presence of neutral to three times ionized tin atoms in the sidelobes close to the target surface. The cross section due to $4d\text{-}\epsilon f$ photoionization for each of these species is in the range of 5–25 MB (≈ 11 MB over the 2% bandwidth)³¹ in the region of the spectrum recorded here, and only changes slowly with increasing energy in this range. Thus the entire spectrum is reduced in intensity in the 9–17 nm region when recorded at angles close to the target surface.

Figures 2 and 3 illustrate the importance of taking the viewing angle into account when assessing and utilizing the EUV emission from a LPP source. The inband output from the targets is higher in both cases at 45°. From these figures an approximation of the angular distribution of the EUV light can be made, assuming a $\cos^n(\theta)$ function. For the pure tin case a value of $n=0.18$ is obtained, while the 5% tin case is more isotropic, with $n=0.14$. These values compare well with the value reported by Shields *et al.*⁹ of $n=0.1$ for Xe plasmas under similar laser illumination conditions to this study. It should be noted that these values would appear to depend heavily on the spot size and laser pulse energy under investigation, as Yamaura *et al.*¹⁴ obtained $n=0.5$ for a pure tin plasma formed from a 500 μm spot size and a 40 J Nd:YAG laser pulse, using the fundamental wavelength.

When the intensity of the spectra is normalized, as shown in Figs. 4 and 5, the influence of plasma opacity on

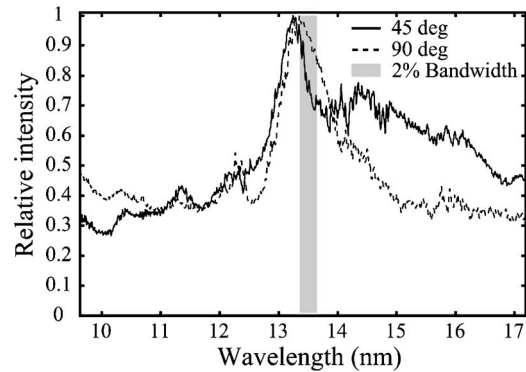


FIG. 4. Normalized emission spectra of plasmas formed from solid tin targets, viewed at angles of 90° and 45° from the laser pulse illumination axis.

the shape of the spectra becomes clearly visible. The spectra of the plasmas formed from the ceramic containing 5% tin (Fig. 5) are almost identical in shape, while those recorded from the pure tin plasmas differ significantly. Considering the pure tin spectra first, it can be seen that at the long wavelength shoulder of the UTA there is a large degree of absorption of the plasma emission in the case of 45° observation. This may be attributed to the presence of relatively hot (4–15 eV) dense plasma in the region outside the hotter inner core responsible for the UTA emission. Here, ions ranging from four to nine times ionized absorb the UTA emission in an almost discrete fashion by $4p\text{-}4d$ and $4d\text{-}4f$ transitions. This interpretation is supported by three factors: (1) the observations of Filevich *et al.*³⁰ who report dense plasma lobes forming at angles around 45° to the laser axis with electron temperatures of approximately 10 eV, (2) preliminary atomic structure calculation using the Cowan code which enables the identification of regions of absorption due to individual ion stages, and (3) by similar observations in the case of spectra of xenon LPP sources³² aided by the emission analysis of a xenon LPP performed by Churilov and Joshi.²² As discussed earlier, the plasmas generated from targets containing 5% tin emit more isotropically than those formed from pure tin targets. This may be ascribed to the lower density of tin in the cool dense sidelobes that form when the ceramic target is irradiated by the EUV radiation from the plasma. Thus a lower level of discrete and continuous absorption occurs at all angles of observation.

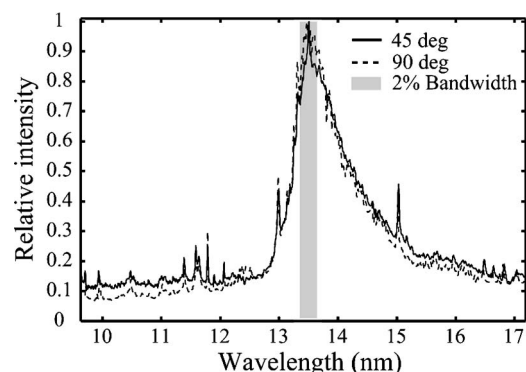


FIG. 5. Normalized emission spectra of plasmas formed from ceramic targets containing 5% tin atoms, viewed at angles of 90° and 45° from the laser pulse illumination axis.

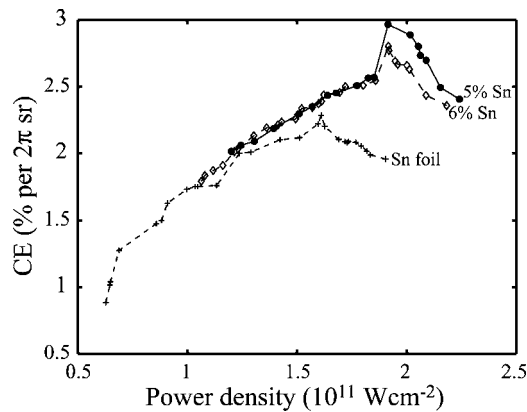


FIG. 6. Conversion efficiency (CE) into 2% bandwidth at 13.5 nm of plasmas formed from pure tin targets and ceramic targets containing 5% and 6% tin atoms, viewed at an angle of 45° from the laser pulse illumination axis.

Figure 6 shows a plot of the CE as a function of power density for three different target types. These are pure tin and two ceramics, one containing 5% tin and the other 6% tin by number. In each case the spot size was fixed at $\sim 180\ \mu\text{m}$, while the power density was varied by changing the laser pulse energy. The data points are recorded at 45° to the laser axis, and the CE figures are calculated assuming that the 45° value is representative of the average inband output of the plasma over a 2π sr solid angle. This results in a slight overstatement of the CE of the plasma under these laser illumination conditions. While the recorded CE is 2.3% for pure tin and 3% for the 5% tin ceramic, when the angular distribution of the EUV emission is taken into account these values become 2.2% and 2.9%, respectively, with an error of 10% on the values reported. These CEs are in agreement with the 1.7%–5% reported from various models.^{33–35} It is noteworthy that the 5% tin target yields the highest CE and that both it and the 6% target yield their highest CE at a higher power density than that required for the pure tin target. This reflects the fact that the electron density and average level of ionization are lower in plasmas containing predominantly low-*Z* elements for a given laser power density.³⁶ Thus a higher power density must be attained in order to reach the level of ionization required to have a sufficiently high density of tin ions with open *d*-shell configurations.

V. CONCLUSION

In conclusion, we have demonstrated that the viewing angle for a laser produced plasma formed from a solid, planar target has an enormous influence on the level of EUV radiation observed in the 2% band at 13.5 nm. In the case of a plasma formed from a pure tin target the radiation is anisotropic in terms of both the spectrum shape and intensity. For plasmas formed from low-*Z* targets containing 5% tin, the shape of the spectrum is almost identical when observed at 90° and 45°, while the intensities recorded vary by a factor of almost 3. These effects must be taken into account when inferring the conversion efficiencies of EUV sources based on laser produced plasmas.

ACKNOWLEDGMENTS

This work was supported by Science Foundation Ireland under Research Grant No. IN/02/199 and by Intel Ireland. The assistance of Professor Mike Morris, at the Department of Chemistry, University College Cork, is gratefully acknowledged for XRF and SEM measurements.

- ¹S. Bajt, J. B. Alameda, T. W. Barbee, W. M. Clift, J. A. Folta, B. B. Kaufmann, and E. A. Spiller, *Proc. SPIE* **4506**, 65 (2001).
- ²P. Hayden *et al.*, *Proc. SPIE* **5826**, 154 (2005).
- ³A. Sasaki, K. Nishihara, F. Koike, T. Kagawa, T. Nishikawa, K. Fujima, T. Kawamura, and H. Furukawa, *IEEE J. Quantum Electron.* **10**, 1307 (2004).
- ⁴G. O'Sullivan and R. Faulkner, *Opt. Eng.* **33**, 3978 (1994).
- ⁵S. Churilov, Y. N. Joshi, and J. Reader, *Opt. Lett.* **28**, 1478 (2003).
- ⁶K. Fahy *et al.*, *J. Phys. D* **37**, 3225 (2004).
- ⁷B. A. M. Hansson and H. M. Hertz, *J. Phys. D* **37**, 3233 (2004).
- ⁸H. Fiedorowicz, A. Bartnik, H. Daido, I. W. Choi, M. Suzuki, and S. Yamagami, *Opt. Commun.* **184**, 161 (2000).
- ⁹H. Shields, S. W. Fornaca, M. B. Petach, M. Michealian, R. D. McGregor, R. H. Moyer, and R. S. Pierre, *Proc. SPIE* **4688**, 94 (2002).
- ¹⁰Y. Tao *et al.*, *Appl. Phys. Lett.* **85**, 1919 (2004).
- ¹¹I. W. Choi *et al.*, *J. Opt. Soc. Am. B* **17**, 1616 (2000).
- ¹²J. R. Hoffman, A. N. Bykanov, O. V. Khodykin, A. I. Ershov, N. R. Bowering, I. V. Fomenkov, W. N. Partlo, and D. W. Myers, *Proc. SPIE* **5751**, 892 (2005).
- ¹³M. Kanouff, H. Shields, L. Bernardez, D. Chenoweth, and G. Kubiak, *J. Appl. Phys.* **90**, 3726 (2001).
- ¹⁴M. Yamaura *et al.*, *Appl. Phys. Lett.* **86**, 181107 (2005).
- ¹⁵U. Stamm *et al.*, *Proc. SPIE* **4688**, 122 (2002).
- ¹⁶D. Colombant and G. F. Tonn, *J. Appl. Phys.* **44**, 3524 (1973).
- ¹⁷J. White, P. Hayden, P. Dunne, A. Cummings, N. Murphy, P. Sheridan, and G. O'Sullivan, *J. Appl. Phys.* **98**, 113301 (2005).
- ¹⁸R. Cowan, *The Theory of Atomic Structure and Spectra* (University of California Press, Berkeley, 1981).
- ¹⁹G. O'Sullivan and P. K. Carroll, *J. Opt. Soc. Am.* **17**, 227 (1981).
- ²⁰P. Mandelbaum, M. Finkenthal, J. L. Schwob, and M. Klapisch, *Phys. Rev. A* **35**, 5051 (1987).
- ²¹C. Bauche-Arnoult and J. Bauche, *Phys. Scr., T* **T40**, 58 (1992).
- ²²S. Churilov and Y. Joshi, *Phys. Scr.* **65**, 40 (2002).
- ²³T. Matsui and N. Kogawa, *Proc. SPIE* **3886**, 610 (2002).
- ²⁴P. Dunne, G. O'Sullivan, and D. O'Reilly, *Appl. Phys. Lett.* **76**, 34 (2000).
- ²⁵K. Ota, EUVL Source Workshop, SEMATECH, Miyazaki, Japan (2004) (unpublished); http://www.semtech.org/resources/litho/meetings/euvl/20041105/02_EUV_Source_Requirements_Ota.pdf
- ²⁶R. L. Kauffman, D. W. Phillion, and R. C. Spitzer, *Appl. Opt.* **32**, 6897 (1993).
- ²⁷A. P. Shevelko, L. A. Shmaenok, S. S. Churilov, R. K. F. Bastiaensen, and F. Bijkerk, *Phys. Scr.* **57**, 276 (1998).
- ²⁸C.-S. Koay, S. George, K. Takenoshita, R. Bernath, E. Fujiwara, M. Richardson, and V. Bakshi, *Proc. SPIE* **5751**, 279 (2005).
- ²⁹D. W. Myers, I. V. Fomenkov, B. A. M. Hansson, B. C. Klene, and D. C. Brandt, *Proc. SPIE* **5751**, 248 (2005).
- ³⁰J. Filevich, J. J. Rocca, E. Jankowska, E. C. Hammarsten, K. Kanizay, M. C. Marconi, S. J. Moon, and V. N. Shlyaptsev, *Phys. Rev. E* **67**, 056409 (2003).
- ³¹M. Lysaght, D. Kilbane, N. Murphy, A. Cummings, P. Dunne, and G. O'Sullivan, *Phys. Rev. A* **72**, 014502 (2005).
- ³²G. O'Sullivan *et al.*, *AIP Conf. Proc.* **771**, 108 (2005).
- ³³T. Aota and T. Tomie, *Phys. Rev. Lett.* **94**, 015004 (2005).
- ³⁴A. Cummings, G. O'Sullivan, P. Dunne, E. Sokell, N. Murphy, and J. White, *J. Phys. D* **38**, 604 (2005).
- ³⁵Y. Shimada *et al.*, *Appl. Phys. Lett.* **86**, 051501 (2005).
- ³⁶A. Cummings *et al.*, *J. Phys. D* **39**, 73 (2005).